1976

Evaluation of Critical Soil Properties Needed to Predict Soil Water Flow Under Desert Conditions

W. A. Jury

L. H. Stolzy

J. Letey Jr.

L. V. Weeks

1975 PROGRESS REPORT
[FINAL]

EVALUATION OF CRITICAL SOIL PROPERTIES NEEDED TO PREDICT SOIL WATER FLOW UNDER DESERT CONDITIONS

W. A. Jury, L. H. Stolzy (Project Leader), J. Letey, Jr.
and L. V. Weeks
University of California, Riverside

US/IBP DESERT BIOME
RESEARCH MEMORANDUM 76-32

in

REPORTS OF 1975 PROGRESS
Volume 3: Process Studies
Abiotic Section, pp. 1-21

1975 Proposal No. 2.3.5.2

Printed 1976

Citation format: Author(s). 1976. Title.
US/IBP Desert Biome Res. Memo. 76-32.
Utah State Univ., Logan. 21 pp.

Ecology Center, Utah State University, Logan, Utah 84322

ABSTRACT

The first phase of the investigation focused on determining the transport coefficients for liquid water movement in desert soils within the IBP validation sites. Hydraulic conductivity and soil water diffusivity were measured for "Rock Valley" gravelly sandy loam and Tuback and Rillito gravelly sandy loams over a soil-water pressure range of —0.05 to —50.00 bars using a transient outflow method. A secondary investigation looked into the possibility of determining the moisture transmission properties of the soils from screened samples from which the stony fraction had been removed.

The major part of the present phase of the investigation was concerned with evaluating heat and water movement under surface rocks in a field soil. Results of a field experiment designed to evaluate the effect of surface rocks on soil heat flow are presented. Temperature observations were made by thermocouples at 12 locations under and adjacent to rocks placed over bare soil. Continuous readings were taken for 24- and 48-hr intervals using seven different kinds of rock cover, ranging from large granite slabs to gravel piles, during the time between December 1974 and August 1975.

Experimental results consistently showed a nonnegligible 24-hr net horizontal heat flow toward the rock at both the 2.5- and 5.0-cm depths. Net vertical heat flow was always downward in the soil under the bare surface but was observed to be either upward or downward in the soil under the rock cover depending on prior conditions. Because water movement in moist soil is generally in the same direction as heat flow, it was suggested that surface rock cover may be a mechanism for water collection in arid climates. To investigate the effect of stones on water movement, rocks were placed at intervals over an initially dry field and left for 6 wk. Subsequent sampling showed a small, but detectable, excess of water stored under the rock compared to adjacent bare soil. Following an irrigation, buried thermal conductivity probes were used to monitor water content changes under and adjacent to surface rocks. After 24 days, the soil under the rock contained significantly more water than did the soil region adjacent to the rock, a finding confirmed by gravimetric sampling. Following this, the stones and probes were relocated for a further 24 days of observation with similar results obtained.

In a separate laboratory experiment using a large, sealed soil column with a rock covering part of the surface, it was demonstrated that a significant amount of water moved to the cylinder of soil under the rock from the soil region under the bare surface due to horizontal temperature gradients induced by the rock covering part of the surface.

Simulation models describing two-dimensional heat flow and water flow in uniform soil under a rectangular rock are discussed. A method is described for correcting the readings of thermal conductivity probes in the field for disturbances due to external soil heating or cooling.

INTRODUCTION

Soil physicists during the last half century have developed and verified transport equations for movement of heat, water and chemicals through a porous medium. The majority of the experimental studies, however, have taken place under carefully controlled laboratory conditions. The benefits of this approach have been numerous. We now possess a detailed theory of soil water movement which has been validated numerous times under conditions of uniformity imposed in laboratory studies.

Application of these models to field studies, however, has met with less universal success because a number of the complications of field properties lie outside the assumptions made in deriving the equations. These complications include lateral variability of soil transport coefficients (Nielsen et al. 1973), soil transport properties which change in time, or perturbations introduced by externally changing environmental variables such as temperature. A basic challenge which must be met by today's soil physicists is to find suitable modifications of these equations which will apply under field conditions, or to determine different ways of looking at the basic problem of transport which might circumvent the need for detailed equations. A "black box" approach to soil water flow would be an example of the latter philosophy (Jury et al., in press).

The purpose of this study was to determine the changes needed in the existing framework to apply soil water flow to desert or semiarid conditions. From a practical standpoint, the most important benefit to be gained from an increased understanding of soil water flow under arid conditions is a better knowledge of how to utilize the existing precipitation by artificial alteration of the soil properties in order to enhance water conservation. This might take the form of surface mulching to restrict evaporative loss, or treatment of the soil surface to cause runoff to a central channeling basin.

In addition to the limitations imposed on extending theories to field conditions, there are several specific characteristics of arid zones which will influence the choice of approach to be used. Arid zones in general are

characterized by conditions wherein the annual potential evapotranspiration (PET) exceeds the annual precipitation. In addition, the precipitation tends to be infrequent, seasonal and unpredictable in magnitude (Mandel 1973). The result of these two influences is a scarcity of vegetative cover existing under natural influences, so that any theory of transport must take into account the bare and dry nature of the surface.

Another important characteristic of arid zone soils is the increased importance of soil temperature. The bare and dry nature of the soil surface results in a much larger component of soil heat flow than would be the case under a moist, covered surface. Under such dry soil conditions the most important mechanism of water transport is through vapor movement and this is known to be greatly influenced by the presence of temperature gradients (Cary 1963). One result of this is a large diurnal cycling of water content changes in the surface layers of the soil due to downward movement of water vapor during the day and upward movement at night (Jackson 1973). This large dependence between water movement and heat flow suggests that a mechanism for water conservation might lie in alteration of normal heat flow patterns. This hypothesis formed a major part of our investigation during the past year.

SUMMARY OF PREVIOUS WORK

The early part of this investigation focused on determining the transport coefficients for liquid water movement in desert soils within the IBP validation sites. Hydraulic conductivity and soil water diffusivity were measured for "Rock Valley" gravelly loamy sand, and Tuback and Rillito gravelly sandy loams over a soil water pressure range of —0.05 to —50.00 bars using a transient outflow method (Mehuys et al. 1975b). A secondary investigation looked into the possibility of determining the moisture transmission properties of the soils from screened samples in which the stony fraction (>2 mm) had been removed. It was found that, when expressed as a function of soil water pressure, hydraulic conductivity values were similar whether or not stones were present. When conductivity was expressed as a function of volumetric water content, the values were higher for a given water content when stones were present. A simple correction of water content of stone-free samples, based on the stone volume of each soil sample, adequately accounted for differences observed when water contents were computed on a total water content basis.

Moisture movement induced by thermal gradients in sealed laboratory soil columns was studied under steady-state conditions. For Tuback and Rillito soils, water content in the soil columns remained unchanged during the experiment due to an initially high water content. In studies with "Rock Valley" soil, thermal moisture diffusivity decreased from 14.0 to 1.3 x 10^3 $cm^2 \cdot hr^{-1} \cdot °C^{-1}$ as water content decreased from 0.14 to 0.08, indicating that much of the moisture movement from hot to cold regions probably occurred in the liquid phase. However, the values of this coefficient were scattered and the influence of stones on the measured values could not be determined from experimental data.

A qualitative evaluation (Mehuys et al. 1975a) was made of the role larger stones may play in the water economy of desert environments by providing vapor condensation surfaces on their underside. Condensation of water vapor could occur whenever the temperature beneath a stone is lower than the dew point temperature. Two laboratory experiments -- one involving a buried stone, the other involving a surface stone -- were set up to measure the temperature distributions under and around stones submitted to a diurnal heat wave. Temperatures were monitored both in air-dried and moist soil. Only when a stone was placed on the surface of air-dried soil were temperatures found to be lower than in the surrounding soil. A maximum difference of 7 C was obtained a few hours after heating began. During the cooling period, the trend was reversed. When soil is sufficiently dry that water moves mainly in the vapor phase, condensation would occur in the early part of the day. This preliminary study suggested that the effect might be an important means of moisture accumulation for desert flora and fauna, so it was decided to pursue the study further in a field experiment the following year.

PRESENT STUDY

Heat and Water Movement Under Surface Rocks in a Field Soil

Soil Temperature and Heat Flux Investigation

The problem of optimizing water use in an arid or semiarid zone is a formidable one for several reasons. Rainfall is generally seasonal, resulting in a large input of water to the soil for a short period of time followed by long stretches when the surface is subjected to a high radiation load and is receiving no water input, unless by artificial irrigation. Desert plant species, in order to survive in such conditions, have evolved shapes to minimize transpirational loss and exhibit markedly seasonal growth and flowering stages (Stark and Love 1969). They have also shown the ability to survive at leaf water potentials as low as —70 bars (Al-Ani et al. 1972).

This impressive drought tolerance suggests that desert plants make use of what water is available in a most efficient way, and it is reasonable to suggest that artificial systems which increase the available water, even if only slightly, will result in a greater prosperity for the plant. An illustration of this is the increase in plant activity frequently found beside desert highways, where the water budget has been improved somewhat by surface runoff.

Another possibility for increasing the available water is through rocks located on or near the soil surface. In addition to acting as a barrier to evaporative loss, the stones could induce lateral movement of heat which could in turn cause

migration of moisture. Stark (1970) considered condensation of water vapor on subsurface rocks to be a major source of water for several desert species studied in Death Valley from March to June. The mechanism proposed was that soil heat flow provided the energy to evaporate dispersed water in the soil, which then concentrated and condensed on the underside of cooler rocks near the surface.

There have been several studies of water vapor movement in the field, but only a few have tried to relate this movement to soil temperature gradients. Rose (1968) used the heat and water flow equations proposed by Philip and deVries (1957) to predict movement of water in liquid and vapor phases while monitoring the surface boundary conditions and measuring gradients in the soil. Jackson and coworkers (Jackson et al., in press; Kimball et al., in press) intensively monitored and sampled a field plot at 0.5-hr intervals and tested the theory of Philip and deVries (1957), finding it predictive only over a small range of water content.

Despite the overall lack of quantitative agreement between theory and experiment, there have been numerous observations suggesting a relationship between water vapor movement and temperature gradients. Letey (1968) examined a large volume of one-dimensional laboratory data and found that all measurements of the vapor flux over a wide range of soil moisture tensions could be explained by the simple flux relation:

$$J_V = -\beta L(T)\, dT/dZ \qquad (1)$$

where L(T) is only a function of temperature and β is a geometric factor usually varying between 1.0 and 2.0.

It is the purpose of this study to investigate the influence of surface stones on collecting subsurface moisture by temperature-induced water vapor movement. This section will discuss the heat flow patterns observed in a field experiment.

Experimental Description—The field study took place at the Botanical Garden of the University of California, Riverside, between December 1974 and August 1975. A level field area was selected, containing a loam (48% sand, 41% silt, 11% clay) in the upper 50 cm. A subplot measuring 3.5 x 3.5 m was cleared of vegetation by a methyl bromide application and 12 copper-constantan thermocouples were planted in a grid at depths of 2.5 and 5.0 cm and on the soil surface in a location partially covered by a rock (Fig. 1). In addition, one thermocouple was epoxied to the rock surface, roughed and colored so as not to alter the energy balance at the rock surface. The thermocouples were connected to an electronic reference junction (Validyne Corp.) and the output fed into a rotating-input chart recorder (Speedomax H, Leeds & Northrup Co.) and monitored for periods of time varying from 24 to 48 hr. Seven different types of stone cover were analyzed over a period of 9 months.

The thermal conductivity λ of the soil as a function of water content was determined by use of a thermal probe similar to that reported by Fritton et al. (1974) on samples of the field soil removed to the laboratory. In the latter part of the field experiment, probes were also buried in the experimental plot to give a direct determination of thermal conductivity. Volumetric heat capacity C was calculated from the water content and particle size distribution by the method suggested by deVries (1966), and thermal diffusivity K_T was calculated as the ratio λ :C.

Table 1 gives a summary of the types of surface cover used, ranging from a large solid rock (40-cm diameter) to a small gravel pile. These were symmetrically placed over the thermocouple grid and the temperature at each location recorded during the period of observation.

Results and Discussion—A typical example of the observations made in the field study is shown in Figure 2, which gives the temperature readings at 2.5 and 5.0 cm under the rock and adjacent bare soil for a 48-hr run on two very hot days in August 1975.

Several general features of the temperature profiles found throughout this experiment are illustrated in this figure. First, although the temperatures at a given depth under the bare soil and under the rock are essentially in phase, the rock acts as an insulator during the hottest hours of the day. Second, the time evolution of the temperature difference between soil and rock at a given depth is asymmetrical, indicating that a net amount of heat is flowing to the stone over a 24-hr period.

From gravimetric water content sampling and use of the laboratory curve of thermal conductivity, estimates were made of the heat flux moving horizontally toward the stone at the 2.5- and 5.0-cm depths and vertically downward at the 3.75-cm depth under the rock and under the bare soil. Table 2 summarizes all the integrated heat flow information for the field study. The values in columns 5 to 8 were obtained from the following:

$$I = \int_0^{24} J_{12}(t)\, dt$$

$$= \sum_{j=1}^{24} J_{12}(t_j)\, \Delta t_j \qquad (2)$$

where

$$J_{12} = -\lambda(\theta)(T_1 - T_2)/\Delta_{12} \qquad (3)$$

is the heat flux between thermocouples at locations 1 and 2, T the temperature, Δ_{12} the distance between thermocouples, t the time in hours and I is the net heat flowing between points 1 and 2 over a 24-hr period.

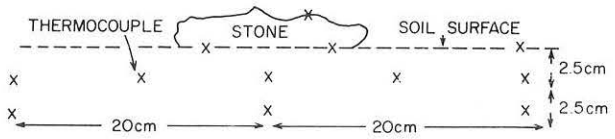

Figure 1. Spatial distribution of thermocouples in the field experiment.

It is of interest to note that with the exception of one cool day in December 1974, all horizontal readings show a net 24-hr flow of heat toward the rock (columns 5 and 6). However, although the vertical heat flux consistently averaged net downward under the bare soil, the flow beneath the rock cover was sometimes upward, reflecting a dependence on prior conditions. This could be caused by the rock shielding the surface from radiation during the hottest hours of the day and also keeping the lower depths warmer at night by insulating the surface against heat loss. Both of these effects could contribute to enhancing water storage underneath the rock.

Theoretical Study—In an attempt to extrapolate information obtained from the field experiments, an effort was made to simulate the heat flow through the soil under and around the rock by a two-dimensional model with symmetrical rectangular geometry (Fig. 3). For this system it is necessary to solve the following equations:

inside the rock,

$$0<x<W, 0<y<D$$

$$C_R(\partial T_R/\partial t) = \lambda_R \nabla^2 T_R \qquad (4)$$

within the soil,

$$0<x<B, -H<y<0$$

$$C_S(\partial T_S/\partial t) = \nabla\cdot(\lambda_S \nabla T_S) \qquad (5)$$

subject to the following boundary conditions:

$$\begin{aligned}
T_S(x, -H) &= T_0, \quad 0<x<B\\
\partial T_S(0, y)/\partial x &= 0, \quad -H<y<0\\
\partial T_S(B, y)/\partial x &= 0, \quad -H<y<0\\
T_S(x, 0) &= T_S(t), \quad W<x<B\\
\partial T_R(0, y)/\partial x &= 0, \quad 0<y<D\\
T_R(x, D) &= T_R(t), \quad 0<x<W\\
T_R(w, y) &= T_R(t), \quad 0<y<D\\
T_S(x, 0) &= T_R(x, 0), \quad 0<x<W\\
\lambda_S T_S(x, 0)/\partial y &= \lambda_R \partial T_R(x, 0)/\partial y, \quad 0<x<W
\end{aligned} \qquad (6)$$

where

T_S = soil temperature (°C)
T_R = rock temperature (°C)
λ_S = soil thermal conductivity (mcal·cm^{-1}·°C^{-1}·sec^{-1})
λ_R = rock thermal conductivity (mcal·cm^{-1}·°C^{-1}·sec^{-1})
C_S = soil volumetric heat capacity (cal·cm^{-1}·°C^{-1})
C_R = rock volumetric heat capacity (cal·cm^{-1}·°C^{-1})
$-H$ = depth of soil affected by the diurnal wave (cm)
B = half the distance between rocks (cm)
W = half the rock width (cm)
D = rock height (cm)
∇^2 = $\partial^2/\partial x^2 + \partial^2/\partial y^2$ (cm^{-2})

The value to use for λ_S must be carefully selected, because the soil thermal conductivity is known to be a function of both soil water content and temperature (deVries 1966). The measurements of λ_S as a function of water content at a temperature of 25 C, determined on packed laboratory samples of the field soil, are shown in Figure 4. It is clear that the value of λ_S will change considerably if a substantial migration of moisture occurs.

The postulated temperature variation of the effective soil thermal conductivity is considered chiefly to be due to the temperature dependence of water vapor movement (Equation 1; deVries 1966). As a first approximation, we could estimate, using Equation 1:

$$\lambda_S(T) = \lambda_S(25\text{ C}) + \beta\,\Delta H\,[L(T) - L(25\text{ C})] \qquad (7)$$

where ΔH is the latent heat of vaporization of water.

To illustrate the simulation, the soil surface and rock surface data for June 25-26 were used to supply $T_S(t)$ and $T_R(t)$, along with the mean measured values for the 0- to 7.5-cm depth of volumetric water content = .025, giving λ_S (25 C) = 0.47 (mcal·cm^{-1}·°C^{-1}·sec^{-1}) and C_S = 0.27 (cal·cm^{-3}·°C^{-1}), and estimated values for the rock of 4.2 (mcal·cm^{-1}·°C^{-1}·sec^{-1}) and C_R = 0.28 (cal·cm^{-3}·°C^{-1}) (Carslaw and Jaeger 1959). Geometric values used were B = 25 cm, H = 25 cm, W = 10 cm and D = 10 cm. The curve for L(T) found in Letey (1968) was approximated by L(T) = .007 exp (.05 T) cm²·day^{-1}·°C^{-1} and β was given the value of 2.0. Equations 4 to 7 were solved without iteration by the finite difference alternating direction implicit technique (Douglas and Peaceman 1955), using a space mesh of 1.25 cm and a time step of 0.25 hr for each half cycle. Three simulations were run using different values for λ_S. The first ignored the influence of vapor movement and set $\lambda_S = \lambda_S$ (25 C) = 0.47 (mcal·cm^{-1}·°C^{-1}·sec^{-1}). The second used a constant λ_S evaluated at T = $(T_{max} + T_{min})/2$, which on this day was 0.84 (mcal·cm^{-1}·°C^{-1}·sec^{-1}) (T = 34 C). The third simulation used Equation 7 with T being the average value of the temperature at the 2.5-cm depth determined each hour. The value of λ_S estimated from Equation 7 was then used for the following hour in Equations 4 to 6. On June 25-26 this resulted in a variation of λ_S from 0.38 to 1.28 (mcal·cm^{-1}·sec^{-1}).

Table 1. Types and characteristics of stone cover used in the field experiments

Stone No.	Description	Color	Diameter (cm)	Thickness (cm)	Texture
1	flat, dense	red	40.0	15.0	smooth
2	uneven, dense	red	30.0	10.0	rough
3	uneven, concrete	gray	10.0	6.0	rough
4	uneven, dense	white	20.0	10.0	smooth
5	gravel pile	gray	10.0	2.0	--
6	flat, concrete	gray	18.0	10.0	rough
7	uneven, dense	red	15.0	5.0	rough

Table 2. Integrated 24-hr summaries of heat flow under various kinds of surface rock cover for a bare field experiment

Date	Rock	Water Content	Thermal Conductivity	Integrated Heat Flux* Horizontal 2.5 cm	Horizontal 5.0 cm	Vertical at 3.75 cm under rock	Vertical at 3.75 cm under soil	Surface Temp. Max	Surface Temp. Min
		cm^3/cm^3	mcal/cm°s	ly or cal/cm^2				°C	°C
12/18	1	.123	1.12	-3.25	-1.83	-5.05	-12.40	18.5	5.5
5/7	2	.030	0.50	10.37	6.48	2.20	14.26	43.5	8.5
5/8	2	.030	0.50	7.94	5.67	-1.94	4.02	48.0	9.5
5/9	2	.030	0.50	11.66	6.93	5.31	6.48	51.0	9.5
5/12	3	.025	0.47	12.64	2.75	5.83	16.72	55.0	11.0
5/13	3	.025	0.47	12.31	1.62	2.60	10.39	54.0	13.5
5/14	4	.025	0.47	9.89	4.43	-3.31	5.79	52.0	12.5
6/25	4	.025	0.47	11.81	6.96	4.76	10.89	57.0	11.5
6/28	5	.025	0.47	6.05	2.57	5.81	3.99	63.0	11.5
6/29	5	.025	0.47	6.26	2.51	5.17	4.45	62.5	11.0
7/22	6	.096	0.94	14.98	3.94	3.63	17.34	46.0	15.5
8/12	7	.032	0.51	12.12	3.18	-3.97	8.74	61.0	14.0
8/13	7	.032	0.51	11.33	2.85	-7.15	5.56	60.0	13.0

* Horizontal flow to the rock and vertical flow downward are positive.

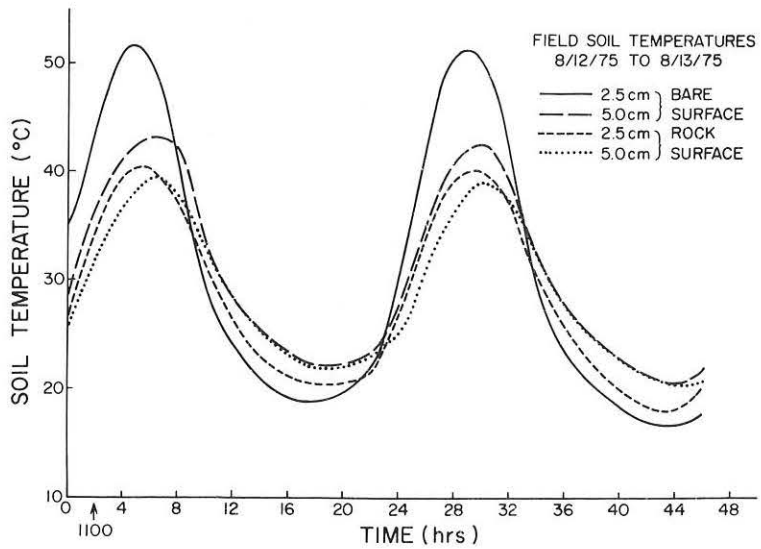

Figure 2. Soil temperature profiles at four locations beneath and around the rock cover 7 on August 12-13, 1975.

The plot of predicted and measured temperatures at the 2.5- and 5.0-cm depths is shown in Figures 5 and 6. The general agreement between predicted and measured values along with the predicted differences between the various models allow several inferences to be made about the nature of heat flow under these circumstances:

1. Failure to compensate the λ_S values determined at 25 C for changes in temperature results in a large error in estimating soil temperature during the hot periods of the day, indicating that water vapor movement was playing a significant role in heat transfer.
2. The variable λ_S simulation does not predict enough soil cooling at night. This could possibly be caused by a failure to account for increasing water content changes in λ_S due to upward water vapor movement at night. An estimate of the amount of water vapor movement expected under these circumstances is made in a paper by Jury and Bellantuoni (in press [c]).
3. The constant λ_S simulation using the average $((T_{max} + T_{min})/2)$ temperature at 2.5 cm does an adequate job of reproducing the data, indicating that single temperature measurements along with a thermal mean estimate of λ_S using Equation 7 may suffice for simple field calculations of heat flow.
4. Considering the number of assumptions made, the agreement between predicted and measured amplitudes and phases for the mean or variable λ_S cases is quite reasonable, indicating that the simulation may be useful in representing heat flow in regions that were not directly monitored in the field experiment.

Summary and Conclusions—The presence of a rock surface cover over bare soil induces lateral heat flow in the soil profile which during the hot summer months results in a net horizontal movement toward the cylinder of soil beneath the rock over a 24-hr period. Also, vertical movement beneath the rock may average net upward or downward even though the vertical movement under bare soil is always net downward in the summer. Since water vapor is known to move under temperature gradients, presence of a rock surface cover suggests a mechanism for water collection and conservation in arid climates. In the following section the movement of water under surface rocks is examined both theoretically and experimentally in detail.

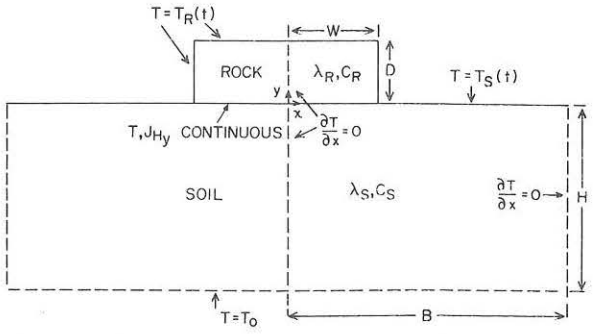

Figure 3. Geometric configuration and boundary conditions for two-dimensional heat flow simulation.

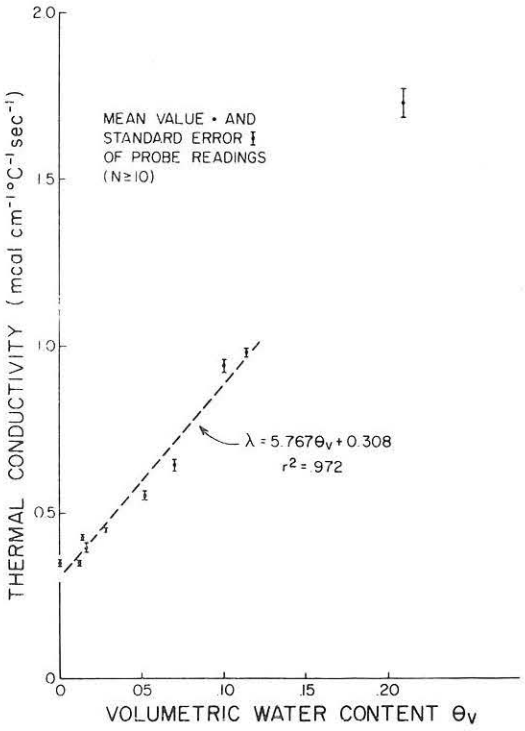

Figure 4. Thermal conductivity vs. volumetric water content at 25 C for field soil used in experiments.

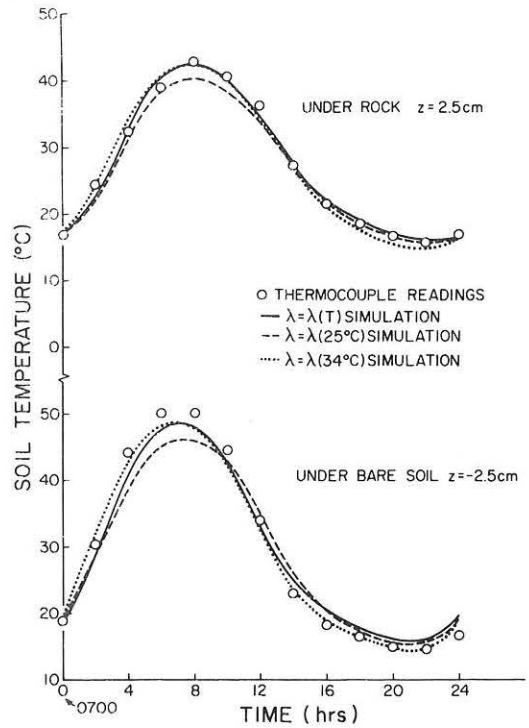

Figure 5. Model predictions and field data at the 2.5-cm depth. Top curve = under rock, bottom curve = under bare soil for variable λ_S (———); constant λ_S at 25 C (------); constant λ_S at T_{ave} (·····).

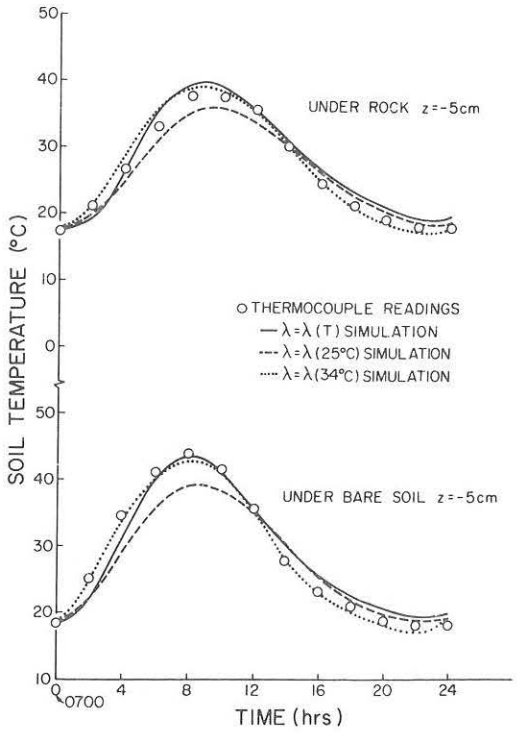

Figure 6. Model predictions and field data at the 5.0-cm depth. Top curve = under rock, bottom curve = under bare soil for variable λ_S (———); constant λ_S at 25 C (------); constant λ_S at T_{ave} (·····).

Water Movement Investigation

In the previous section the authors reported on heat flow measurements made in a field experiment under and around rocks covering bare soil. Having consistently observed a net lateral movement of heat toward the soil under the rocks on a 24-hr basis in the summer months, we reasoned that accompanying movement of water due to thermal gradients, primarily in the vapor phase, could result in a net deposit of moisture under the rocks which would then be insulated from evaporative loss.

Testing this hypothesis in a field environment, however, is quite difficult for several reasons. A nondestructive monitoring of soil water content, normally achieved by using tensiometers or soil psychrometers, is complicated by the large daily change in soil temperatures experienced at the locations of interest. Destructive gravimetric soil sampling is achieved only by replicating across the field and results in a one-time-only comparison between soil under and adjacent to the rock. Also, comparison between rocks sampled at different times is greatly hampered by lateral variability in field properties. Further, the highly dynamic and three-dimensional nature of the heat flow patterns suggests that larger water content measuring instruments (i.e., gamma ray transmission) buried in the soil might perturb the thermal environment sufficiently to cause unwanted influences on water movement. Because of these limitations, it was decided to try using buried thermal conductivity probes (deVries and Peck 1958), supplemented by gravimetric sampling, to study the patterns of water accumulation and movement in rock-covered soil. Appendix I gives a brief description of the procedures used to adapt the probe to the experiment.

Experiment Description—The field used in the water movement studies is the same 3.5 x 3.5 m subplot described above. In the first experiment (May 6 to June 24, 1975), the field was initially sampled for water content at four locations and three depth intervals (0-7.5, 7.5-15 and 15-22.5 cm), and then four medium-sized rocks (flat, 25-cm diameter, 10-cm thickness) were placed on the surface at random locations across the field. Occasional sampling under and around the rocks was accomplished by lifting up the rock, taking out the plug of soil and replacing it with a core taken from another part of the field, and then putting the rock back in place. Subsequent samples under the rock were taken at different locations in the covered area. A second experiment (July 1-24, 1975) was initiated by removing all rocks, irrigating the field and then replacing the rocks in new locations. Separate tests showed that the soil under the rocks wet up thoroughly after an irrigation, so the rocks were placed on the field after the conclusion of the water input on July 1. In addition, three thermal conductivity probes (Fritton et al. 1974) were planted horizontally at the 5-cm depth under and around one of the rocks. Thermal conductivity λ was measured occasionally and related to water content θ from the laboratory-determined curve of $\lambda(\theta)$ (Fig. 4). Final soil samples were taken under and around the other rocks on July 24. The probes and rocks were then moved to other parts of the field and a third observation period initiated without an irrigation (July 25 to August 22, 1975).

One experiment was conducted under controlled laboratory conditions to attempt to study the water movement under and around a rock in the absence of surface evaporation. A sample of fine desert sand from the playa in Jornada, New Mexico, was sieved with a 2-mm screen, mixed to a volumetric water content of 0.10 (cm^3/cm^3) and packed as uniformly as possible to a bulk density of 1.4 (g/cm^3) in a large (56-cm diameter, 12.7 cm deep) plastic circular tub with a sealed bottom. A flat marble slab (25 x 10 x 2 cm) was centered on the surface with thermocouples located on the top of the slab, on the soil surface under and 10 cm adjacent to the rock. In addition, two thermal conductivity probes were buried at the 5-cm depth, one extending under the rock and one 10 cm adjacent to the rock. A thin plastic sheet was laid over the soil surface except at the rock location and a thin layer of dry soil was spread over the top of it. The bottom of the tub was laid on a surface of circulating water kept at 35 $\pm$ 1 C by cooling coils connected to a constant temperature reservoir (Forma-Temp). The soil surface was exposed to four heat lamps run from a variable voltage input to permit variation of surface radiation exposure. The setup of this experiment is shown in Figure 7.

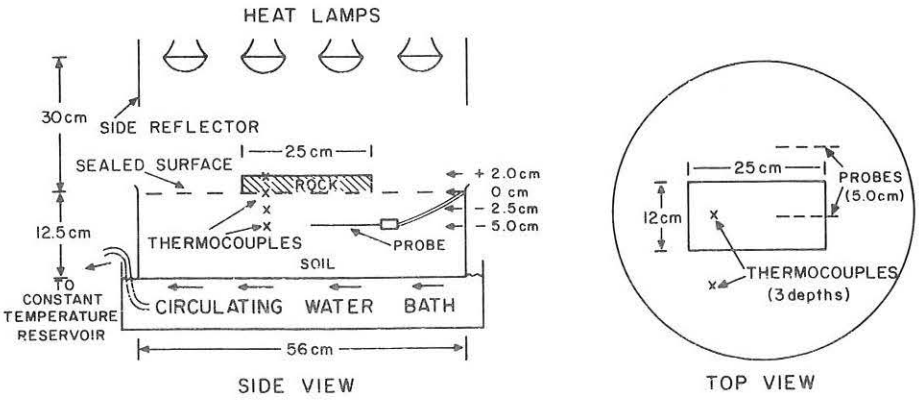

Figure 7. Laboratory soil column used to study water movement under surface rocks. A buried plastic sheet on the soil surface prevents evaporative loss.

Theoretical Analysis—To supplement the field measurements of water content changes in the vicinity of surface rocks, a simulation model was constructed to try to estimate the amount of water vapor movement expected to occur under the changing thermal profiles measured in the field (Jury and Bellantuoni, in press [a]).

Simulation of water vapor movement in soil is very difficult owing to the possibility of phase changes and complicated interaction within liquid and vapor regions (Philip and deVries 1957). Transient flow of water in the vapor phase may be described by the species continuity equation (deVries 1958):

$$(\partial \theta / \partial t)v + \underset{\sim}{\nabla} \cdot \underset{\sim}{J}_v = E \qquad (8)$$

where

J_v = rate of flow of water vapor per area per time (cm liq·cm^{-3}·sec^{-1})
θ_v = volumetric liquid equivalent of vapor (cm^3 /cm^3)
E = rate of change of liquid to vapor/soil volume (cm^3·cm^{-3}·sec^{-1})

The evaporation term E is a function of the vapor pressure of the liquid phase in the medium, which is in turn determined by temperature and the relative humidity of the surrounding vapor. The flux term J_v will in general be driven by gradients of vapor density, which, for fairly wet soil, may be represented by a general equation:

$$\underset{\sim}{J}_v = -\beta L(T) \underset{\sim}{\nabla} T \qquad (9)$$

where L(T) is a vapor transport coefficient and β is a geometric factor.

Letey (1968) applied Equation 9 to a large variety of laboratory data from the literature and found the measurements could be represented by a single function $L(T) \sim .007 \exp(.05T)$ (cm^2·day^{-1}·°C^{-1}) with β ranging between 1.0 and 2.0.

As a crude estimate of the net amount of water vapor transport expected to occur according to Equations 8 and 9, one could ignore phase changes and calculate changes in water storage according to

$$\partial \theta_v / \partial t = \nabla \cdot h\beta L(T) \nabla T \qquad (10)$$

where $h = 1$ for $\theta_v > 0$ and $h = 0$ for $\theta_v = 0$.

This is tantamount to assuming that the medium consists of vapor and solid matrix only and that the vapor will redistribute according to changes in density induced by temperature gradients.

Equation 10 was coupled to the output of the two-dimensional temperature simulation in rock-covered soil described in the previous section, together with the boundary conditions which were

1. no vertical flow of vapor across soil surface,
2. no horizontal flow of vapor across rock midpoint plane and soil plane midway between rocks, and
3. no vertical flow of vapor at Z = —25 cm.

Conditions 1 and 3 correspond to a sealed surface and bottom while 2 follows from symmetry arguments. Evaporation was suppressed in order to isolate the influence of temperature gradients on soil water content changes.

Results and Discussion—The first experimental period (May 6 to June 24) was monitored by gravimetric sampling only and was conducted on a very dry field which received no external water input at any time. The initial gravimetric water content θ_g averages for the four samples taken on May 11 were: .021 $\pm$ .004; .035 $\pm$ .005; and .036 $\pm$ .005 (g/g) at

the depths of 0-7.5, 7.5-15 and 15-22.5 cm, respectively. The amount of variation in water content across the field was deemed sufficient to restrict comparisons in water accumulation to samples taken of soil under and immediately adjacent to a given rock.

Table 3 shows the difference in gravimetric water content between soil under and adjacent to rocks recorded at the 0-7.5 cm depth as a function of time. The results, although consistently showing more water underneath the rocks, do not show any pattern of water accumulation. In view of the inherent errors of sampling, profile replacement and field variability, they must be regarded as inconclusive.

The second experiment was designed to test the response of a rock-strewn system to an external water application. Figure 8 shows the readings of the thermal conductivity probes as a function of time after irrigation, adjusted for temperature fluctuations by the method of Jury and Bellantuoni (in press [b]) and related to water content using the curve from another study by Jury and Bellantuoni (in press [a]). Probe 1 was located along the center line of a 25-cm diameter rock, probe 2 was 5 cm from the south edge and probe 3 was 10 cm from the north edge; all probes were buried at 5-cm depth. Measurements were made in the morning before the soil heated up, and several readings were taken at each location. These tended to agree within 10% or better if the first measurement was omitted. This first reading deviated significantly from the others and was considered to be inaccurate, possibly due to contamination from dew formation on the probe.

Figure 8 suggests that all regions were heavily depleted by drainage during the first day following irrigation, that the exposed regions subsequently lost water by evaporation, and illustrates the ability of rock cover to conserve water collected after a precipitation. This is also shown in Table 4, which summarizes the final analysis (July 24) of water content under and around the two other rocks on the field.

Following this analysis, the probes were checked and moved, along with the rocks, to another part of the field and observed for another 24 days, a period marked by intense radiation; the average maximum air temperature for the period was 35 C. Figure 9 shows the output of probe 1, planted right at the edge of the rock, and of probe 2, located 10 cm away. The pattern of drying again is different in the region near the rock, which loses water less rapidly than the bare soil surface region. The final soil sampling across the field confirmed that bare soil and rock-covered areas were both losing water. Table 5 shows the profile for these areas, which were bare from July 1-24 and rock covered thereafter.

Although these results demonstrate the effectiveness of rocks in water retention, they do not shed any light on the influence of thermal gradients in concentrating water under rocks. The column experiment (Fig. 7) was devised to look at changes in water content caused by temperature gradients in the absence of evaporation. The heat lamps were turned on and thermal conductivity probe measurements taken with background temperature compensation (Appendix I) for 5 hr, after which the lamps were turned off. Figure 10 is a plot of the probe readings under the rock and adjacent to the rock, along with a plot of the temperature gradient at the 2.5-cm depth ($(T_{soil} - T_{rock})/15$ cm).

This figure definitely shows substantial movement of water over a short period of time in the same direction as the lateral component of heat flux. Further, it is suggestive that the region under the rock accumulated water until the horizontal temperature gradient reversed, and then began to lose water.

Simulation Results—Figure 11 is a plot of the volumetric water content, assumed initially to be 0.10, as a function of time at three depths for a three-day simulation. This was obtained by using the field surface temperature data for June 25, 1974, in the two-dimensional heat flow calculation and calculating the water content changes with Equation 10, assuming no loss through the surface. The rock and soil readings are taken 1.25 cm inside and outside of the rock edge, respectively. The simulation is a vast oversimplification, particularly as it ignores phase changes and liquid flow, but it does point out the size of changes in water storage to be expected from pure vapor movement in a rock-covered soil environment. The most dramatic changes occur near the surface where the temperature gradients are largest, but there is, in addition, a net lateral transfer of moisture to the rock induced by lateral temperature gradients, similar to that observed in the sealed column experiment.

Conclusions—The series of field and laboratory measurements taken in this study illustrate the effectiveness of surface rocks in helping retain water in the soil profile underneath. Evidence for the ability of the rocks to create thermal patterns which help to concentrate water from the adjacent soil underneath the rocks was indirectly observed through field temperature measurements which consistently showed a net horizontal movement toward the soil, directly observed in a laboratory experiment, and calculated in a simulation of water vapor movement.

There are several potentially important aspects of the process of heat and water movement in soil which were not isolated in this study but may, nevertheless, make significant contributions to the retention of water in a rock-covered soil:

1. The largest changes in water content on a daily basis occur very near the surface. Jackson (1973) observed a bare field for several weeks following an irrigation and observed a diurnal change in volumetric water content of the 0-0.5 cm layer from 0.24 to 0.09 and back to 0.19 on the fifth day after irrigation.
2. If the rock underside at the soil surface is cooler than the immediate soil environment, condensation of migrating water vapor could result which would further enhance the patterns of concentration.

3. Water in the liquid phase also moves in response to temperature gradients. Although traditionally thought to be unimportant on a short-time scale, recent measurements have shown the transport coefficient for thermally induced liquid transport to be many times larger than predicted from the accepted theoretical model (Jury and Miller 1974).

One final point worth mentioning is that the lateral temperature gradients would be induced by any surface feature which shaded part of the soil, such as an isolated creosotebush in the desert, and thermally aided water transport may be a previously overlooked method of moisture collection for arid zone vegetation.

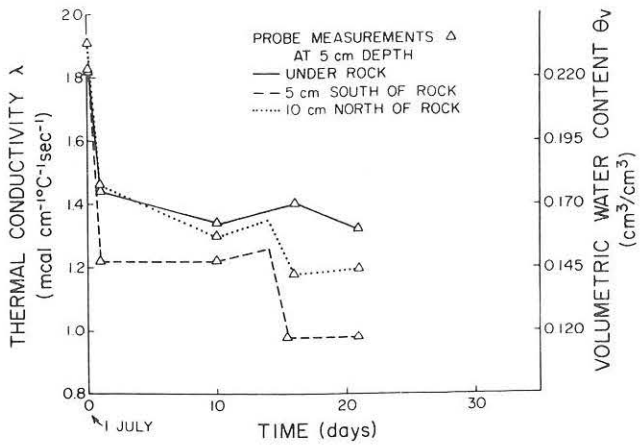

Figure 8. Thermal conductivity readings as a function of time after irrigation at the 5-cm depth: ——— = under; ------ = 5 cm south; ····· = 10 cm north of a surface rock of 25-cm diameter during the July 1-24, 1975, experiment.

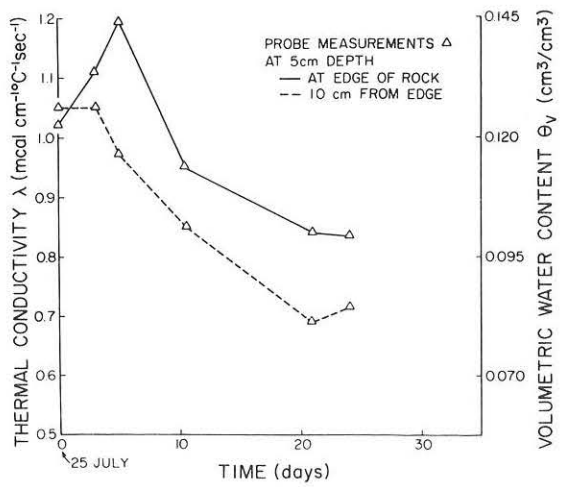

Figure 9. Thermal conductivity readings as a function of time at the 5-cm depth: at the edge (———); 10 cm from the edge of a surface rock of 25-cm diameter (------) during the July 25 to August 15 experiment.

Table 3. Differences (rock minus soil) in gravimetric water content of the 0 to 7.5 cm depth between rock-covered and adjacent bare surface soil measured on an initially dry field (average θ g = .021 (g/g))

Date	Location of Rock			
	1	2	3	4
5/16	.007	.010	*	*
5/23	.002	.012	*	*
6/2	.003	.010	.005	.005
6/9	.009	.008	.003	.003
6/24	.003	.000	.002	.001

* No samples taken

Table 4. Gravimetric water content profiles under and adjacent to surface rock cover (20-cm diameter), 24 days after an irrigation of the bare field

Depth	Area 1		Area 2	
	Rock	Soil	Rock	Soil
0 to 7.5	.061	.035	.048	.044
7.5 to 15	.061	.056	.076	.060
15 to 22.5	.070	.071	.078	.068

Table 5. Gravimetric water content profiles under and adjacent to surface rock cover (20-cm diameter), 28 days after rock placement on previously bare soil

Depth	Area 3		Area 4	
	Rock	Soil	Rock	Soil
0 to 7.5	.024	.019	.022	.020
7.5 to 15	.037	.033	.043	.036
15 to 22.5	.048	.048	--	.052

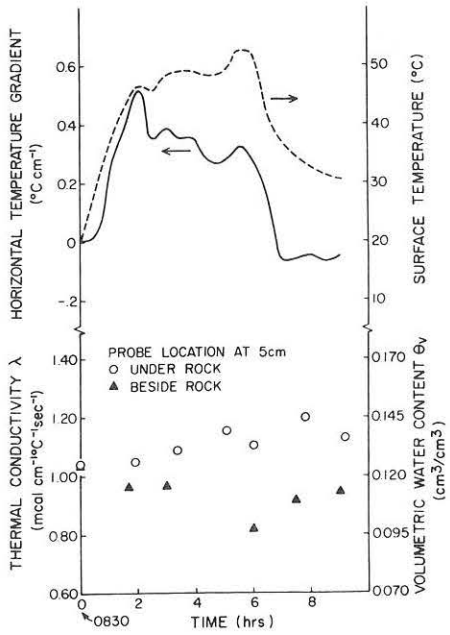

Figure 10. Thermal conductivity readings as a function of time at the 5-cm depth: open circles = under the rock; triangles = 10 cm adjacent to the rock edge, along with the horizontal temperature gradient at the 2.5-cm depth and the surface temperature for the sealed column experiment.

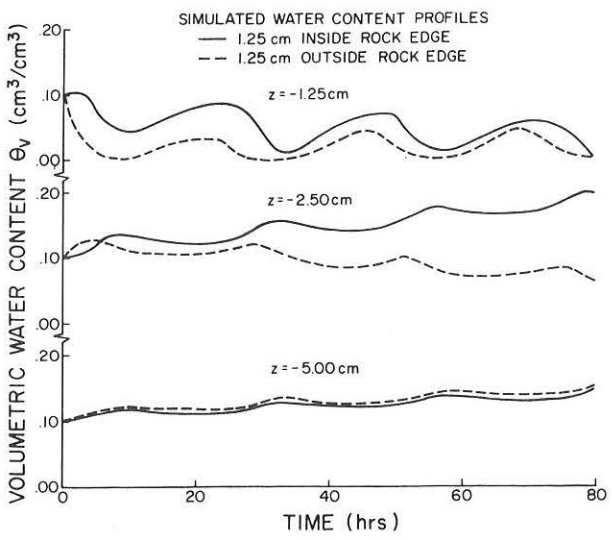

Figure 11. Simulated water content profiles caused by vapor movement induced by temperature gradients: 1.25 cm under rock edge (———); 1.25 cm outside rock edge (------).

LITERATURE CITED

Al-Ani, H. A., B. R. Strain, and H. A. Mooney. 1972. The physiological ecology of diverse populations of the desert shrub *Simmondsia chinensis*. J. Ecol. 60:41-57.

Carslaw, H. S., and J. C. Jaeger. 1959. Conduction of heat in solids, 2nd ed. Oxford Univ. Press, London. 509 pp.

Cary, J. W. 1963. Onsager's relation and non-isothermal diffusion of water vapor. J. Phys. Chem. 67:126-129.

deVries, D. A. 1958. Simultaneous transfer of heat and moisture in porous media. Trans. Amer. Geophys. Union 39:909-915.

deVries, D. A. 1966. Thermal properties of soils. *In* W. R. Van Wijk, ed. Physics of plant environment. North-Holland Publ. Co., Amsterdam.

deVries, D. A., and A. J. Peck. 1958. On the cylindrical probe method of measuring thermal conductivity with special reference to soils. I. Extension of theory and discussion of probe characteristics. Aust. J. Phys. 11:255-271.

Douglas, J., and D. W. Peaceman. 1955. Numerical solution of two-dimensional heat flow problems. AIChE Bull. 1:505-512.

Fritton, D. D., W. J. Busscher, and J. E. Alpert. 1974. An inexpensive but durable thermal conductivity probe for field use. Soil Sci. Soc. Amer. Proc. 38:854-855.

Hadas, A. 1974. Problems involved in measuring the soil thermal conductivity and diffusivity in a moist soil. Agr. Meteorol. 13:105-113.

Jackson, R. D. 1973. Diurnal changes in soil water content during drying. *In* Field soil water regime. Soil Sci. Soc. Amer. Spec. Publ. 5.

Jackson, R. D., R. J. Reginato, B. A. Kimball, and F. S. Nakayama. Diurnal soil-water evaporation: comparison of measured and calculated soil-water fluxes. Soil Sci. Soc. Amer. Proc. (In press)

Jury, W. A., and B. Bellantuoni. A background temperature correction for thermal conductivity probes. Soil Sci. Soc. Amer. Proc. (In press [a])

Jury, W. A., and B. Bellantuoni. Heat and water movement under surface rocks in a field soil. I. Thermal effects. Soil Sci. Soc. Amer. Proc. (In press [b])

Jury, W. A., and B. Bellantuoni. Heat and water movement under surface rocks in a field soil. II. Moisture effects. Soil Sci. Soc. Amer. Proc. (In press [c])

JURY, W. A., W. R. GARDNER, P. G. SAFFIGNA, and C. B. TANNER. Model for predicting simultaneous movement of nitrate and water through a loamy sand. Soil Sci. (In press)

JURY, W. A., and E. E. MILLER. 1974. Measurement of the transport coefficients for coupled flow of heat and moisture in a medium sand. Soil Sci. Soc. Amer. Proc. 38:551-557.

KIMBALL, B. A., R. D. JACKSON, R. J. REGINATO, F. S. NAKAYAMA, and S. B. Ioso. Diurnal soil-water evaporation: comparison of measured and calculated soil-heat fluxes. Soil Sci. Soc. Amer. Proc. (In press)

LETEY, J. 1968. Movement of water through soil as influenced by osmotic pressure and temperature gradients. Hilgardia 39:405-418.

MANDEL, S. 1973. Hydrology of arid zones. *In* B. Yaron, E. Danfors, and Y. Vaadia, eds. Arid zone irrigation. Springer-Verlag, Berlin and New York. 434 pp.

MEHUYS, G. R., L. H. STOLZY, and J. LETEY. 1975a. Temperature distributions under stones submitted to a diurnal heat wave. Soil Sci. 120(6):437-441.

MEHUYS, G. R., L. H. STOLZY, J. LETEY, and L. V. WEEKS. 1975b. Effect of stones on the hydraulic conductivity of relatively dry desert soils. Soil Sci. Soc. Amer. Proc. 39:37-42.

NAGPAL, N. K., and L. BOERSMA. 1973. Air entrapment as a possible source of error in the use of a cylindrical heat probe. Soil Sci. Soc. Amer. Proc. 37:828-832.

NIELSEN, D. R., J. W. BIGGAR, and K. T. ERH. 1973. Spatial variability of field-measured soil-water properties. Hilgardia 42:215-260.

PHILIP, J. R., and D. A. DEVRIES. 1957. Moisture movement in porous materials under temperature gradients. Trans. Amer. Geophys. Union 38:222-232.

ROSE, C. W. 1968. Water transport in soil with a daily temperature wave. Aust. J. Soil Res. 6:31-44.

STARK, N. 1970. Water balance of some warm desert plants in a wet year. J. Hydrol. 10:113-126.

STARK, N., and L. D. LOVE. 1969. Water relations of three warm desert species. Isr. J. Bot. 18:175-190.

WIERENGA, P. J., D. R. NIELSEN, and R. M. HAGEN. 1969. Thermal properties of a soil based upon field and laboratory measurements. Soil Sci. Soc. Amer. Proc. 33:354-360.

APPENDIX I

Use and Calibration of the Thermal Conductivity Probe

Introduction

Thermal conductivity probes have been in use for many years as a method of determining the thermal conductivity (λ) of soils under controlled laboratory conditions with precise temperature controls. With a few exceptions, however (Wierenga et al. 1969), they do not seem to have been used extensively in the field.

The probe is basically a shielded wire which is heated by passing current through it. A thermocouple is attached for measuring the resulting temperature rise. This temperature rise is a function of the thermal conductivity of the surrounding soil.

There are several difficulties involved with the probe measurement which would, of course, be compounded in the field. Hadas (1974) analyzed the influence of poor contact between probe and soil and showed that large errors in the determination of λ may result, particularly for measurements made at higher water contents. Nagpal and Boersma (1973) looked at the effects of air entrapment and concluded that it could cause thermal conductivity underestimates of a factor of 1.8 in wet soil. deVries and Peck (1958) looked at theoretical modifications resulting from the finite size of the probe and concluded that the simple theory assuming a line source may be used if the probe is well packed. They also suggested that a number of temperature measurements be used in the slope determination. Their analysis of moisture migration due to temperature gradients set up by the probe showed that this would have a negligible influence on the determination of λ if the heating current was low.

Unfortunately, there are several requirements of the probe for field use which are in conflict with the above. Thin probes are too fragile for insertion into compacted field soils and several of the thicker glass-encased models are also difficult to maintain. A recently proposed design (Fritton et al. 1974) has been altered to be durable enough for field use, but this has been achieved by making the diameter 0.65 cm, which results in finite effects on the temperature profile which differ from the simple theory. For this reason, early time temperature readings must be either corrected or disregarded.

Thus, use of the probe in a practical application has many difficulties. Heat generated by the probe should be kept small to avoid perturbing the medium, but must be large enough to be discernible over backgound temperature fluctuations. Similarly, although heating time should be kept short, it must be long enough to offset the influence of the probe size and to allow time for several distinct readings of temperature to be made. Times of 120-180 sec of heating are typical (deVries and Peck 1958), with at least the first 30 sec not being used.

These limitations are compounded even further in field applications, because the soil is warming or cooling due to the diurnal radiation cycle, and the probe thermocouple is continuously reacting to these background changes. During periods of rapid soil temperature change (e.g., mid-morning), probe readings taken would cause great errors in determining λ unless a very large probe heating current were used, and this in itself would introduce errors due to moisture migration. This paper outlines a simple in situ probe reading correction which can be made on readings from small heating currents to compensate for external fluctuations, and demonstrates its effectiveness in correcting thermally biased laboratory determinations of thermal conductivity.

Theory

The simplified theory for the thermal conductivity probe is based on the solution to the cylindrical heat flow equation:

$$C(\partial T/\partial t) = (\lambda/r)(\partial/\partial r)[r(\partial T/\partial r)] \qquad (I\text{-}1)$$

for a constant line source of heat q (energy/length), constant thermal conductivity λ and heat capacity C, infinite medium and uniform initial temperature T. For these conditions the solution of Equation I-1 (Carslaw and Jaeger 1959) may be written:

$$T - T_0 = q/4\pi\lambda[-E_i(-r^2/4kt)] \qquad (I\text{-}2)$$

where $k = \lambda/C$ is the thermal diffusivity and E is the exponential integral.

For all but the smallest times, Equation I-2 expands to

$$T - T_0 = q/r\pi\lambda(-\gamma + \ln 4k/r^2 + \ln t) \qquad (I\text{-}3)$$

so that a plot of $T - T_0$ vs. ln t should have as slope $q/4\pi\lambda$ where $q = I^2R$, with I the uniform current and R the resistance/length of the probe.

In practice, determination of this slope can be quite error prone, and as many readings of $T - T_0$ as possible should be taken to determine it. If the soil is also being warmed from above, however, as in the morning hours in the field, this heating will be attributed to the line source and will cause a large error in the determination of the slope. For heating currents small enough to avoid water movement, we experienced errors of up to 50 % trying to use the probes in soil at the 7.5-cm depth.

As a compensation for this, we decided to try and determine the average background warming or cooling of the soil around the probe, called background temperature $T_B(t)$, and subtract this from the probe temperature during a run, so that

$$T - T_0 - T_B(t) = q/4\pi\lambda[-\gamma + \ln(4k/r^2) + \ln t] \qquad (I\text{-}4)$$

Strictly, this is not a valid superposition, because Equation 2 is the solution of Equation I-1 only for the case of uniform medium temperature. Nevertheless, Equation I-4 may be approximately true and could represent an improvement over Equation I-3 for time-varying soil temperature.

The simplest way to estimate T(t) is to observe the temperature change at the thermocouple for a period of time (we used 90-120 sec) without turning on the heater current. The resultant data (which may be scattered) are fit to a linear regression:

$$T_B(t) = a\,t + \beta \qquad \text{(I-5)}$$

Another method for obtaining $T_B(t)$ is to mount a thermocouple in the soil at the same depth as the probe thermocouple and record the temperature continuously for several minutes preceding and following the times when the probe is being heated. This curve will generally be smoother, but may represent a different thermal environment than that of the probe thermocouple.

To test the value of the correction against an absolute standard, a controlled laboratory experiment was run on an oven-dried soil.

Experimental Procedure

Two thermal conductivity probes were packed in containers filled with screened (2-mm sieve), oven-dried sandy loam taken from a desert site at Jornada, New Mexico. One probe was packed horizontally to a depth of 5.0 cm in an insulated rectangular box. A copper-constantan thermocouple was buried at the same depth about 5 cm from the probe and a second thermocouple was planted at the surface. The other probe was placed vertically into an insulated cylinder filled with the sand so that the end of the probe and the wires extruded from the surface over the probe. A copper-constantan thermocouple was located about 5 cm laterally from the probe. A second thermocouple recorded surface temperatures.

Each container, in separate experiments, was placed below a heat lamp which was turned on for several hours and then extinguished. Background temperature recordings were made continuously from the reference thermocouple, and preceding each probe heating by a 90-sec observation of the probe thermocouple. Probe heating runs were made at 10- to 20-min intervals by a constant voltage power supply (Staco, Inc.). Temperature rise was recorded at 15-sec intervals by observation of a nanovoltmeter (Kiethley Instruments) over a 180-sec heating cycle, during which time the temperature rise at the probe surface was about 1.0 C. The temperature vs. logarithm of time data slope (Equation I-3 or I-4) between 45 and 180 sec was determined by regression.

Results

The results of the experiments are shown in Figure I-1 (horizontal probe) and Figure I-2 (vertical probe). The circles in each case represent the uncorrected probe readings and the triangles the values corrected for background temperature, determined by plotting the prerun a values (Equation I-5) as a function of time and interpolating between points to determine the correction at the time of a probe run. The solid lines represent the mean values of λ ($0.42 \pm .01$ mcal·cm^{-1}·sec^{-1} for horizontal; $0.46 \pm .01$ mcal·cm^{-1}·sec^{-1} for vertical) taken during isothermal pre- and postexperimental runs. The vertical column was packed to a slightly higher bulk density to help insure good probe-soil contact when the probe was inserted vertically, and so gave a higher initial thermal conductivity value.

It is obvious that the correction technique does an excellent job of reducing background interference, even under the unrealistic heat exposure of the horizontal experiment. The vertical heat input was reduced until the surface temperature maximum was typical of summer bare soil values, and represents more of a field simulation.

Use of a reference thermocouple to determine background temperature was more successful in the horizontal case than in the vertical, as shown in Table I-1, which gives the standard error of the estimate from the true predetermined value for all runs made during the experiment. The explanation for this is probably due to the presence of the probe altering the vertical flow of heat and thus differing thermally from the adjacent soil.

Application to Field Studies

We have used probes in the field and estimated the thermal correction by both techniques described above, with a resulting improvement in consistency and reproducibility of readings (Jury and Bellantuoni, in press [a]). However, we found it advisable to take several reference runs at the probe to insure that a true pattern is picked up, and not just a local perturbation. Furthermore, measurements should be taken at a time when the soil temperature is not changing drastically and when sporadic external fluctuations caused by partial cloudiness or gust winds are not present.

When these precautions are taken it should be possible to use the probe readings as a nondestructive measurement of soil water content θ, providing that the dependence of λ on θ is known. This method would have the advantage of responding rapidly to changes in θ and in remaining calibrated (with the above correction) during times of changing soil temperature.

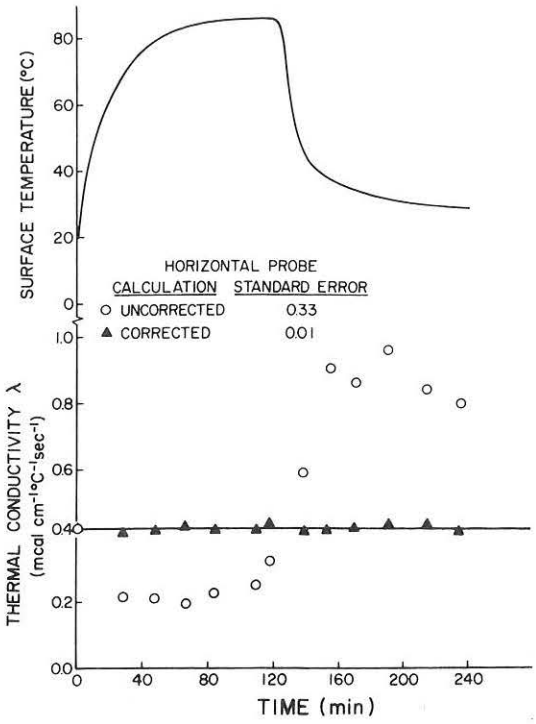

Appendix I, Figure 1. Original and corrected thermal probe readings for horizontal probe position.

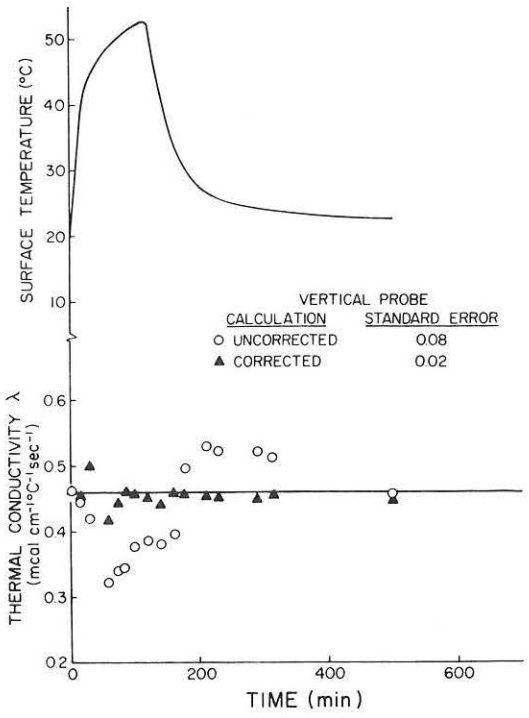

Appendix I, Figure 2. Original and corrected thermal probe readings for vertical probe position.

Appendix I, Table 1. Standard error S_λ of thermal conductivity measurements made during an external temperature change (mcal·cm^{-1}·°C^{-1}·sec^{-1})

$$S_\lambda = \left[\sum_{i=1}^{N} (\bar{X}-X_i)^2/(N-1)\right]^{\frac{1}{2}}$$

	Vertical Probe N = 16	Horizontal Probe N = 13
Uncorrected readings	0.08	0.33
Prerun correction	0.02	0.01
Reference correction	0.03	0.10

APPENDIX II

Computer Program and Documentation

The calculations used in this year's study consisted of solving the two-dimensional heat flux equation for a uniform soil profile with a rectangular stone overlying part of the surface. The temperature distribution was then used to estimate water movement in the vapor phase.

The method of solution of the differential equations was the Alternating Direction Implict (ADI) scheme proposed by Douglas and Peaceman (1955). For an equation with x and y dependence, the solution is advanced ½ time step by treating the y term as a past difference and solving the remaining problem (in x) as an implicit finite difference solution. The result is then advanced another ½ time step, this time in the y direction.

To illustrate, we look at the simple heat flow equation:

$$K(\partial^2 T/\partial x^2 + \partial^2 T/\partial y^2) = \partial T/\partial t \qquad \text{(II-1)}$$

which becomes, in the ADI scheme:

First ½ step:

$$-T(J+1,K,N+\tfrac{1}{2}) - T(J-1, K, N+\tfrac{1}{2}) + (2+W)T(J,K,N+\tfrac{1}{2}) = T(J,K+1,N) + T(J,K-1,N) - (2-W)T(J,K,N) \qquad \text{(II-2)}$$

Second ½ step:

$$-T(J,K+1,N+1) - T(J,K+1,N+1) + (2+W)T(J,K,N+1) = T(J+1,K,N+\tfrac{1}{2}) + T(J-1,K,N+\tfrac{1}{2}) - (2-W)T(J,K,N+\tfrac{1}{2}) \qquad \text{(II-3)}$$

where (J,K,N) are the (x,y,t) nodes and $W = \Delta x^2/kt$ ($\Delta x = \Delta y$).

Generalizations of Equations II-2 and II-3 are written for the stone and soil regions and solved by the standard tridiagonal matrix reduction.

After the T(x,y,t) profiles are generated, they are used to estimate water movement in the following way. It is assumed that

$$(\partial \theta/\partial t) + \underset{\sim}{\nabla} \cdot \underset{\sim}{J}_{vap} = 0 \qquad \text{(II-4)}$$

represents an upper bound to movement of water in the vapor phase. The vapor flux J_{vap} is represented by the approximate relation:

$$\underset{\sim}{J}_{vap} = -h(\theta)L(T)\ \underset{\sim}{\nabla}\ T \qquad \text{(II-5)}$$

where

$$h(\theta) = 0, \quad \theta = 0$$
$$= 1, \quad \theta \gtrsim 0 \qquad \text{(II-6)}$$

is the relative humidity, and

$$L(T) = A\exp(BT) \qquad \text{(II-7)}$$

is an exponential approximation to the general vapor transport coefficient reported by Letey (1968).

To further simplify the computation, the transformation:

$$R(T) = \int_0^T L(T)\, dT$$
$$= A/B[\exp(BT) - 1] \qquad \text{(II-8)}$$

is used with the result:

$$J_{vap} = -h(\theta)\nabla R \qquad \text{(II-9)}$$

Combining II-4, II-9 and the explicit difference approximation gives θ (J,K,N+1) from θ (J,K,N) and T(J,K,N).

List of Subroutines

1. TRID—performs the tridiagonal inversion of the one-dimensional difference equations.
2. VK—calculates the vapor flux RV from the soil temperature profile.

Array List

1. ST(J)—stone surface temperature, hourly increments.
2. SO(J)—soil surface temperature, hourly increments.
3. TX(J,K,N)—stone temperature, past and present time.
4. TG(J,K,N)—soil temperature, past and present time.
5. RV(J,K)—water vapor flux.
6. OT(J,K)—volumetric water content.
7. RH(J,K)—relative humidity.
8. D,E,F—arrays used in equation solution.

Program Listing

MAIN

```
C***THIS PROGRAM SOLVES FOR THE SOIL AND STONE TEMPERATURES AS A FUNCT-
C***ION OF SPACE AND TIME FOR THE CASE OF A STONE LYING ON THE SURFACE
C***OF A UNIFORM SOIL
C***B IS HALF THE DISTANCE BETWEEN THE STONE MIDPOINTS
C***W IS HALF THE WIDTH OF THE STONE
C***H IS THE DISTANCE FROM SOIL SURFACE TO THE ISOTHERMAL DEPTH
C***S IS THE HEIGHT OF THE STONE ABOVE THE SURFACE
C***DELX,DELT ARE THE SPACE AND TIME STEP SIZES (UNSCALED)
C***TDRAT IS THE RATIO STONE/SOIL OF THERMAL DIFFUSIVITIES
C***AL IS A DIMENSIONLESS CONSTANT USED IN THE BOUNDARY CONDITIONS
C***TDSOIL IS THE THERMAL DIFFUSIVITY OF THE SOIL
0001          DIMENSION ST(25),SO(25),K(23,25)
0002          READ(5,1)B,W,H,S,DELX,DELT,TCR,TDROK,TDRAT
0003          READ(5,1)(ST(J),J=1,25)
0004          READ(5,1)(SO(J),J=1,25)
0005     1    FORMAT(10F7.3)
0006          JTM=1
0007          CEVA=0.
C***FORMING DIMENSIONLESS GROUPS
0008          DX=DELX/B
0009          DT=TDROK*DELT/B/B
0010          DT=DT/24.
0011          WW=DX*DX/DT
C***MESHLIMITS
0012          IM=B/DELX
0013          IN=H/DELX+1.
0014          IS=S/DELX+1.
0015          INM2=IN-2
0016          IQ=IS+IN-1
0017          IP=W/DELX
0018          INP1=IN+1
0019          IMP1=IM+1
0020          IPP2=IP+2
0021          IMM1=IM-1
0022          IMP2=IM+2
0023          INM1=IN-1
0024          IQM1=IQ-1
0025          IPP1=IP+1
0026          IPM1=IP-1
0027          ISM1=IS-1
C***TG IS THE SOILTEMPERATURE MATRIX
C***TS IS THE STONE TEMPERATURE MATRIX
0028          DIMENSION TS(23,15,2),D(30),E(30),F(30)
0029          COMMON TG(23,25,2),RV(23,25),DT(23,25),RH(23,25)
0030          DIMENSION HS(25),HF(25)
0031          NP=1
0032          NQ=2
C***INITIALIZATION
0033          DO 2 J=1,IMP2
0034          DO 2 K=1,IN
0035          RV(J,K)=0.
0036     2     TG(J,K,NP)=18.0
0037          DO 3 J=1,IPP1
0038          DO 3 K=1,IS
0039     3     TS(J,K,NP)=18.0
0040          DO 300 J=1,IM
0041          DO 300 K=1,IN
0042     300   DT(J,K)=0.10
0043          DO 502 K=1,IN
0044     502   HS(K)=0.
C***BEGIN FIRST ADI PASS UPDATING SOIL TEMPERATURES
0045          TIME=DT
0046     23   TAVE=(TG(6,INM2,NP)+TG(14,INM2,NP))/2.
0047          TCS=.66-0.03*TAVE+0.001*TAVE*TAVE
0048          TDSOIL=308.*TCS
0049          CK=TDROK/TDSOIL
0050          BE=WW*CK
0051          AL=TCR/TCS
0052          DO 4 K=2,INM1
0053          DO 5 J=2,IMP1
0054     5    D(J)=TG(J,K-1,NP)+(BE-2.0)*TG(J,K,NP)+TG(J,K+1,NP)
0055          F(2)=D(2)/(2.0+BE)
0056          E(2)=2.0/(2.0+BE)
0057          B=2.0+BE
0058          CALL TRID(D,E,F,B,IM+1,3)
0059          TG(IM+1,K,NQ)=(F(IM)+D(IM+1)/2.0)/(1.0+BE/2.0-E(IM))
0060          DO 40 J=1,IMM1
0061          JM=IM-J+1
0062     40    TG(JM,K,NQ)=E(JM)*TG(JM+1,K,NQ)+F(JM)
0063          TG(1,K,NQ)=TG(3,K,NQ)
0064     4    TG(IM+2,K,NQ)=TG(IM,K,NQ)
0065          DO 6 K=2,ISM1
```

```
0066            DO 7 J=2,IP
0067          7   D(J)=TS(J,K-1,NP)+(BE/CK-2.)*TS(J,K,NP)+TS(J,K+1,NP)
0068            E(2)=2.0/(2.0+BE/CK)
0069            F(2)=D(2)/(2.0+BE/CK)
0070            B=2.0+BE/CK
0071            CALL TRID(D,E,F,B,IP,3)
              C***BOUNDARY CONDITIONS...SIDE OF STONE
0072            TS(IP+1,K,NQ)=ST(JTM)
0073            DO 36 J=1,IPM1
0074            JM=IP-J+1
0075         36 TS(JM,K,NQ)=E(JM)*TS(JM+1,K,NQ)+F(JM)
0076          6 TS(1,K,NQ)=TS(3,K,NQ)
              C***BOUNDARY CONDITIONS....TOP OF STONE
0077            DO 8 J=1,IPP1
0078          8   TS(J,IS,NQ)=ST(JTM)
0079            DO 9 J=1,IMP2
0080          9 TG(J,1,NQ)=25.0
              C***BOUNDARY CONDITIONS...STONE-SOIL INTERFACE
0081            DO 10 J=1,IP
0082            TG(J,IN,NQ)=(TG(J,IN-1,NQ)+TS(J,2,NQ)*AL)/(1.0+AL)
0083         10 TS(J,1,NQ)=TG(J,IN,NQ)
              C***BOUNDARY CONDITIONS...SOIL SURFACE
0084            DO 11 J=IPP2,IMP2
0085         11   TG(J,IN,NQ)=SO(JTM)
0086            TG(IPP1,IN,NQ)=ST(JTM)
0087            TS(IP+1,1,NQ)=TG(IP+1,IN,NQ)
              C***BEGIN SECOND ADI PASS
0088            TIME=TIME+DT
0089            NR=NP
0090            NP=NQ
0091            NQ=NR
0092            DO 12 J=2,IP
0093            DO 13 K=1,INM1
0094         13 D(K)=TG(J-1,K,NP)+(BE-2.0)*TG(J,K,NP)+TG(J+1,K,NP)
0095            E(1)=0.
0096            F(1)=25.0
0097            B=2.0+BE
0098            CALL TRID(D,E,F,B,IN-1,2)
              C***BOUNDARY CONDITIONS....TOP OF STONE
0099            E(IN)=AL/(1.0+AL-E(IN-1))
0100            F(IN)=F(IN-1)/(1.0+AL-E(IN-1))
0101            DO 14 K=INP1,IQM1
0102            KR=K-IN+1
0103         14 D(K)=TS(J-1,KR,NP)+(BE/CK-2.)*TS(J,KR,NP)+TS(J+1,KR,NP)
0104            B=2.0+BE/CK
0105            CALL TRID(D,E,F,B,IQM1,INP1)
0106            TS(J,IS,NQ)=(ST(JTM)+ST(JTM+1))/2.
              C***BOUNDARY CONDITIONS...STONE-SOIL INTERFACE
0107            DO 15 K=2,IS
0108            KR=IS-K+1
0109            KT=IN+KR-1
0110         15   TS(J,KR,NQ)=TS(J,KR+1,NQ)*E(KT)+F(KT)
0111            TG(J,IN,NQ)=TS(J,1,NQ)
0112            DO 12 K=1,INM1
0113            KT=IN-K
0114         12   TG(J,KT,NQ)=TG(J,KT+1,NQ)*E(KT)+F(KT)
0115            DO 16 J=IPP1,IMP1
0116            DO 17 K=1,INM1
0117         17 D(K)=TG(J-1,K,NP)+(BE-2.0)*TG(J,K,NP)+TG(J+1,K,NP)
0118            E(1)=0.
0119            F(1)=25.0
0120            B=2.0+BE
0121            CALL TRID(D,E,F,B,IN-1,2)
              C***BOUNDARY CONDITIONS...SOIL SURFACE
0122            TG(J,IN,NQ)=(SO(JTM)+SO(JTM+1))/2.
0123            TG(IPP1,IN,NQ)=(ST(JTM)+ST(JTM+1))/2.
0124            DO 16 K=1,INM1
0125            KT=IN-K
0126         16 TG(J,KT,NQ)=TG(J,KT+1,NQ)*E(KT)+F(KT)
              C***BOUNDARY CONDITIONS...SIDE OF STONE
0127            DO 18 K=1,IS
0128            TS(IP+1,K,NQ)=(ST(JTM)+ST(JTM+1))/2.
0129         18 TS(1,K,NQ)=TS(3,K,NQ)
0130            DO 25 K=1,IN
0131            TG(1,K,NQ)=TG(3,K,NQ)
0132         25 TG(IM+2,K,NQ)=TG(IM,K,NQ)
0133         20   FORMAT(1X,20(1X,F5.2))
0134            TM=TIME*DELT/DT
0135            WRITE(6,21)TIME,TM
0136            DO 19 K=1,ISM1
0137            KK=IS-K+1
0138         19   WRITE(6,20)(TS(J,KK,NQ),J=1,IPP1)
0139              WRITE(6,20)(TS(J,1,NQ),J=1,IP),(TG(J,IN,NQ),J=IPP1,20)
0140            DO 22 K=1,INM1
0141            KK=IN-K
0142         22   WRITE(6,20)(TG(J,KK,NQ),J=1,20)
0143            WRITE(6,20)TG(6,IN-2,NQ),TG(14,IN-2,NQ),TG(6,IN-4,NQ),TG(14,IN-4,
                1NQ),TGS,TDSOIL
```

```
0144              DO 500 K=1,IN
0145         500   HF(K)=(TG(IP+2,K,NQ)-TG(IP,K,NQ))/2.5
0146              WRITE(6,20)(HF(K),K=1,IN)
0147              DO 501 K=1,IN
0148         501   HS(K) =HS(K)+HF(K)
0149              WRITE(6,20)(HS(K),K=1,IN)
0150         21   FORMAT(1H1,16H MACHINE TIME = F9.5,13H REAL TIME = F9.5,6H HOURS)
0151         90    JTM=JTM+1
0152              TIME=TIME+DT
0153         91   IF(JTM-24)68,68,69
0154         69     JTM=1
0155         68     NR=NP
0156              NP=NQ
0157              NQ=NR
0158              GM=TIME*DELT/DT/24.
0159              IF(GM-1.0)23,23,24
0160         24    STOP
0161              END
```

TRID

```
0001              SUBROUTINE TRID(D1,E1,F1,B1,MX,MN)
0002              DIMENSION D1(50),E1(50),F1(50)
0003              DO 30 KA=MN,MX
0004              F1(KA)=(D1(KA)+F1(KA-1))/(B1-E1(KA-1))
0005         30   E1(KA)=1.0/(B1-E1(KA-1))
0006              RETURN
0007              END
```

VK

```
0001              SUBROUTINE VK(LM,LN,LQ)
0002              COMMON TQ(23,25,2),RQ(23,25) ,DQ(23,25),RP(23,25)
0003              DO 400 L=1,LM
0004              DO 400 M=1,LN
0005              IF(DQ(L,M))401,401,402
0006         401   RP(L,M)=0.
0007              GO TO 400
0008         402   RP(L,M)=1.
0009         400   RQ(L,M)=.0114*( EXP(.0546*TQ(L,M,LQ))-1.)
0010              RETURN
0011              END
```

APPENDIX III

Measurement of Thermal Properties

Although the heat and water flow study was concentrated at the botanical garden field site at UCR, samples of desert soils were taken from IBP validation sites at Rock Valley and Jornada. These were returned to the lab and the thermal conductivity, heat capacity and thermal diffusivity were measured or calculated as a function of water content.

Thermal conductivity was determined by the cylindrical heat probe method described in the main body of this report and in Appendix I. The soil samples were sieved with a 2-mm screen and packed to a dry bulk density of 1.4 into cylindrical soil cans (12-cm diameter; 23-cm depth). Wet samples were premixed with water before packing to insure uniformity. The probe was carefully inserted into the can and a series of heating and cooling runs taken to determine values for thermal conductivity λ.

Heat capacity was determined from a formula proposed by deVries (1966) which calculates the volumetric heat capacity of a soil sample as the sum of the contributions due to minerals, organic matter, liquid and gaseous constituents, according to

$$C = C_w X_w + C_M X_M + C_o X_o \qquad \text{(III-1)}$$

where X_w is the volumetric water fraction; X_M is the volumetric mineral fraction; and X_o is the volumetric organic matter fraction; and the gaseous contribution has been neglected.

Using the handbook values for the specific heats of the various materials results in the final equation:

$$C = 0.46 X_M + 0.60 X_o + X_w \text{ cal}\cdot\text{cm}^{-3}\cdot\text{C}^{-1} \qquad \text{(III-2)}$$

The thermal diffusivity k_T was not measured directly but was calculated from the ratio λ :C.

Table III-1 is a summary of all measurements taken for the three soils.

Appendix III, Table 1. Soil thermal properties for botanical garden (BG), Rock Valley (RV) and Jornada Playa (PL) sites

Field site	Vol. water content (cm^3/cm^3)	Bulk density (gm/cm^3)	Thermal conductivity (mcal/cm/ C/sec)	Heat capacity (cal/cm^3/ C)	Thermal diffusivity (cm^2/day)
B.G.	.000	1.4	0.35	0.27	112
	.014	1.4	0.43	0.28	133
	.028	1.4	0.45	0.30	130
	.046	1.4	0.55	0.32	151
	.070	1.4	0.64	0.34	163
	.115	1.4	0.98	0.38	220
	.210	1.4	1.73	0.48	311
	.470	1.4	2.53	0.94	233
RV	.000	1.4	0.37	0.26	123
	.030	1.4	0.44	0.29	131
	.080	1.4	0.56	0.34	142
	.150	1.4	0.81	0.41	171
	.200	1.4	1.21	0.46	227
	.300	1.4	1.81	0.56	279
	.470	1.4	3.07	0.93	285
PL	.00	1.4	0.40	0.26	133
	.01	1.4	0.42	0.27	134
	.02	1.4	0.49	0.28	151
	.04	1.4	0.47	0.30	135
	.08	1.4	0.73	0.34	186